ARTHRITIS & RHEUMATOLOGY
Vol. 69, No. 3, March 2017, pp 655–667
DOI 10.1002/art.39938

In Vivo Role of Neutrophil Extracellular Traps in Antiphospholipid Antibody–Mediated Venous Thrombosis

He Meng,[1] Srilakshmi Yalavarthi,[1] Yogendra Kanthi,[2] Levi F. Mazza,[1] Megan A. Elfline,[1] Catherine E. Luke,[1] David J. Pinsky,[1] Peter K. Henke,[1] and Jason S. Knight[1]

Objective. **Antiphospholipid syndrome (APS) is a leading acquired cause of thrombotic events. Although antiphospholipid antibodies have been shown to promote thrombosis in mice, the role of neutrophils has not been explicitly studied. The aim of this study was to characterize neutrophils in the context of a new model of antiphospholipid antibody–mediated venous thrombosis.**

Methods. **Mice were administered fractions of IgG obtained from patients with APS. At the same time, blood flow through the inferior vena cava was reduced by induction of stenosis. Resulting thrombi were characterized for size and neutrophil content. Circulating factors and the vessel wall were also assessed.**

Results. **As measured by both thrombus weight and thrombosis frequency, mice treated with IgG from patients with APS (APS IgG) demonstrated exaggerated thrombosis as compared with control IgG–treated mice. Thrombi in mice treated with APS IgG were enriched for citrullinated histone H3 (a marker of neutrophil extracellular traps [NETs]). APS IgG–treated mice also demonstrated elevated levels of circulating cell-free DNA and human IgG bound to the neutrophil surface. In contrast, circulating neutrophil numbers and markers of vessel wall activation were not appreciably different between APS IgG–treated mice and control mice. Treatment with either DNase (which dissolves NETs) or a neutrophil-depleting antibody reduced thrombosis in APS IgG–treated mice to the level in control mice.**

Conclusion. **These data support a mechanism whereby circulating neutrophils are primed by antiphospholipid antibodies to accelerate thrombosis. This line of investigation suggests new, immunomodulatory approaches for the treatment of APS.**

Antiphospholipid syndrome (APS), which has an estimated prevalence of at least 1 in 2,000, is a leading acquired cause of both thrombosis and pregnancy loss (1). Approximately half of cases are diagnosed in the background of systemic lupus erythematosus (SLE), while the remaining cases represent a stand-alone syndrome called primary APS (2). In contrast to other prothrombotic diatheses, APS is associated with myriad other clinical complications including thrombocytopenia, skin ulcerations, nephropathy, seizure disorder, cognitive decline, and accelerated atherosclerosis (3). Importantly, these non-clotting manifestations may continue to progress despite treatment with anticoagulation, which is the current standard of care for the management of APS.

With the goal of identifying novel pathways that might be amenable to targeted treatments beyond anticoagulation, there have been efforts to model APS in mice (4). Numerous studies have involved a model of femoral vein pinch injury, whereby infusion of IgG from patients with APS (APS IgG) leads to exaggerated thrombosis (5–7). Additionally, previous studies relied on laser-induced injury to the cremaster microcirculation (8,9) or ferric chloride application (10), in which, again, the presence of APS IgG accelerates the clotting phenotype. Notably, these models relied on direct vessel wall injury, which has unclear relevance for some human

Supported by the Arthritis National Research Foundation (grant ORCID 0000-0003-0995-9771) and the Joshua (Jim) and Eunice Stone Foundation. Dr. Kanthi's work was supported by the NIH (grant K08-HL-131993). Dr. Knight's work was supported by the NIH (National Institute of Arthritis and Musculoskeletal and Skin Diseases grant K08-AR-066569) and by a career development award from the Burroughs Wellcome Fund.

[1]He Meng, MD, PhD, Srilakshmi Yalavarthi, MS, Levi F. Mazza, Megan A. Elfline, MS, Catherine E. Luke, LVT, David J. Pinsky, MD, Peter K. Henke, MD, Jason S. Knight, MD, PhD: University of Michigan Medical School, Ann Arbor; [2]Yogendra Kanthi, MD: University of Michigan Medical School and Ann Arbor Veterans Administration Healthcare System, Ann Arbor.

Address correspondence to Jason S. Knight, MD, PhD, University of Michigan, Department of Internal Medicine, 5520A MSRB1, 1150 West Medical Center Drive, SPC 5680, Ann Arbor, MI 48109. E-mail: jsknight@umich.edu.

Submitted for publication January 22, 2016; accepted in revised form September 15, 2016.

events such as venous thrombosis (the most common manifestation of APS) (11).

Historically, 3 cell types (endothelial cells, platelets, and monocytes) have received the majority of attention as perpetuators of APS-related thrombosis (12). This important work has demonstrated that antiphospholipid antibodies bind to proteins such as β_2-glycoprotein I (β_2GPI), which are associated with cell surface phospholipids (13). This engagement leads to cell activation and up-regulation of prothrombotic molecules such as tissue factor. In particular, a 2-hit hypothesis has been put forth, whereby the endothelium exists in a primed state in patients with APS, while a second event, such as infection, then tips the patient toward thrombosis (14,15).

More recently, our group and others have posited a role for neutrophils in APS (16–18). This work was spurred by a new emphasis in the literature regarding the importance of neutrophils in pathologic clotting and especially venous thrombosis (19). Neutrophils release extracellular chromatin-based structures, coined neutrophil extracellular traps (NETs), through a process known as NETosis (20,21). NETs consist primarily of DNA and histones that originate from the nucleus but also are decorated with cytoplasm-derived material, such as the granule proteins neutrophil elastase and myeloperoxidase. Although NETs were originally characterized for their role in host defense against microbes (20,21), more recent work has suggested an additional role in thrombosis.

The DNA component of NETs can activate the intrinsic coagulation cascade (22,23). Histones stimulate platelets (24), while NET-derived proteases inactivate certain anticoagulant factors (22). In some contexts, NETs may even be an important source of tissue factor (25). Our work with human cells has shown that IgG isolated from patients with APS, and perhaps especially IgG anti-β_2GPI, engages with neutrophils to stimulate NETosis (16). This correlates with more cell-free DNA and NETs in the circulation of patients with APS, even in the absence of acute thrombotic events (16). Another group of investigators has shown that NETs in patients with APS, when formed, may be particularly resistant to degradation by serum DNase (17). Further, low-density granulocytes, neutrophils that are prone to exaggerated NETosis, are found in increased numbers in patients with APS (18).

In this study, we sought to develop a murine model of APS venous thrombosis induced by flow restriction through the inferior vena cava (IVC). As described in the literature, and also as observed in our investigations, this model results in thrombus formation in <50% of control mice (17,22,26). In contrast, the rate of thrombosis is 80–90% when mice are administered APS IgG. The aim of the current study was to characterize neutrophils in this model.

PATIENTS AND METHODS

Human subjects. Patients were recruited from the Rheumatology and Hematology clinics at the University of Michigan. All patients with APS fulfilled the laboratory and clinical requirements for APS established by the Sydney classification criteria (27), while none of the patients met the American College of Rheumatology (ACR) criteria for SLE (28). Healthy volunteers were recruited through a posted flyer; exclusion criteria included history of a systemic autoimmune disease, active infection, and pregnancy. Blood was collected by phlebotomist-performed venipuncture, and serum was prepared by standard methods and stored at −80°C until used. IgG, IgM, and IgA anti-β_2GPI, as well as IgG anticardiolipin and IgM antibodies, were determined by enzyme-linked immunosorbent assay (ELISA) (Inova Diagnostics). Lupus anticoagulant (LAC) was tested according to published guidelines (29).

Preparation of human IgG. IgG was purified from serum samples obtained from APS patients or controls, using protein G–agarose according to the manufacturer's instructions (Pierce). Briefly, serum was diluted in IgG binding buffer and repeatedly (at least 5 times) passed through a protein G–agarose column. IgG was eluted with 0.1*M* glycine and then neutralized with 1*M* Tris. This was followed by overnight dialysis against phosphate buffered saline at 4°C. After passage through a 0.2μ filter, IgG purity was verified by sodium dodecyl sulfate–polyacrylamide gel electrophoresis (SDS-PAGE) and Coomassie staining. IgG concentrations were determined by BCA Protein Assay (Pierce). All IgG preparations were confirmed to be free of endotoxin contamination as determined by a chromogenic endotoxin quantification kit (Pierce).

Animal housing, surgery, and treatments. Mice were housed in a specific pathogen–free barrier facility and fed standard chow. Male C57BL/6 mice (000664) were purchased from The Jackson Laboratory and used at ~10 weeks of age. Peripheral leukocyte and platelet counts were determined with an automated Hemavet 950 counter (Drew Scientific).

Male wild-type C57BL/6 mice were administered 2 doses (500 μg each) of either control or APS IgG by intraperitoneal injection, 48 hours apart. Just prior to the second IgG treatment, a laparotomy was performed, and a ligature was fastened around the IVC over a blunted 30-gauge needle (which served as a spacer). After removal of the spacer, the abdomen was closed, and the mouse was allowed to recover. Here, we will refer to this procedure as the "stenosis" or "flow restriction" model. Sham procedures followed the same protocol, except the ligature was passed under the IVC and then removed from the mouse without fastening. Some mice were additionally treated with DNase (Pulmozyme [dornase alfa]) (Genentech) immediately after surgery, 50 μg by intraperitoneal injection and 10 μg by intravenous (tail vein) injection. Other mice were treated with 2 doses (50 μg each) of anti–Ly-6G antibody (InVivoPlus anti-mouse Ly-6G; BioXCell); these doses were administered 72 and 24 hours before laparotomy was performed. The mice were humanely killed, and thrombus formation was assessed 6 and 48 hours after laparotomy.

In addition to the stenosis model, we also performed a procedure that we here refer to as the "stasis" model; this was done essentially as previously described (30). Briefly, mice underwent complete ligation of the IVC and all visible contributing vessels below the renal veins. This procedure produces

full stasis. The stasis model is well characterized and consistently (>97% of the time) produces a thrombus (30). The stasis model differs from the stenosis model in that 1) the IVC is fully ligated and 2) all visible side and back branches are also ligated.

Venous ultrasound following IVC stenosis. Anesthetized mice underwent laparotomy, and IVCs were sonographically analyzed in vivo by B-mode and color Doppler with a Vevo2100 40-MHz transducer and software (VisualSonics), as previously described (31).

Neutrophil purification and NETosis assay. Bone marrow neutrophils were isolated as previously described (32). Briefly, total bone marrow cells were spun on a discontinuous Percoll gradient (52%, 69%, 78%) at 1,500*g* for 30 minutes. Cells from the 69%–78% interface were collected. These cells were >95% Ly-6G positive as determined by flow cytometry and had typical nuclear morphology as demonstrated by microscopy. To assess in vitro NETosis, a protocol similar to what we have described previously was used (33). IgG stimulation was performed for 4 hours at 37°C in RPMI medium supplemented with 2% bovine serum albumin and 10 m*M* HEPES buffer. Stimulation with phorbol myristate acetate (100 n*M*; Sigma) was also performed for 4 hours.

For immunofluorescence analysis, cells were fixed with 4% paraformaldehyde. DNA was stained with Hoechst 33342 (Invitrogen), while protein staining was performed with rabbit polyclonal antibodies to myeloperoxidase (Dako) or citrullinated histone H3 (Cit-H3) (Abcam), followed by fluorescein isothiocynate–conjugated anti-rabbit IgG (SouthernBiotech). Images were collected with an Olympus IX70 microscope and a CoolSNAP HQ2 Monochrome camera (Photometrics) with MetaMorph Premier software (Molecular Devices). NETs (decondensed extracellular DNA costaining with either myeloperoxidase or Cit-H3) were quantified in a blinded manner by 2 observers and digitally recorded to prevent multiple counts. The percentage of NETs was calculated after counting ten 400× fields per sample.

Thrombus sectioning and immunohistochemistry. At 6 hours and 48 hours, thrombi were easily separated from the vessel wall. Formalin-fixed thrombus sections were stained with a rabbit polyclonal antibody against Cit-H3 (Abcam) and a horseradish peroxidase–conjugated anti-rabbit secondary antibody (Jackson ImmunoResearch). Prior to antibody staining, epitope retrieval was achieved by boiling for 30 minutes in sodium citrate buffer. Color change was detected with a DAB-Plus Substrate Kit (Invitrogen). Images were captured with a BioTek Cytation 5 fitted with Olympus 4× and 20× objectives and, when necessary, stitched together using the associated BioTek software. Positively stained surface area was quantified with ImageJ software.

Western blotting. After separation from the vessel wall, thrombi were prepared for SDS-PAGE by sonication in radioimmunoprecipitation assay buffer (50 m*M* Tris, pH 8.0, 200 m*M* NaCl, 0.5% Nonidet P40, and a Roche protease inhibitor cocktail pellet). Lysates were then cleared by centrifugation at 14,000*g* for 10 minutes at 4°C. Supernatant protein concentrations were measured with a Pierce BCA Protein Assay Kit according to the manufacturer's instructions. Samples were resolved by 15% SDS-PAGE under denaturing conditions and transferred to a 0.45μ nitrocellulose membrane. Primary antibodies were directed against Cit-H3 and histone H3 (both from Abcam). Detection was performed with IRDye-labeled secondary antibodies (Rockland). Images were captured and analyzed with an Odyssey imaging system (Li-Cor).

ELISA for soluble P-selectin. Plasma was tested with a Mouse Soluble P-Selectin/CD62P Quantikine ELISA Kit (R&D Systems) according to the instructions of the manufacturer.

RNA preparation and quantitative polymerase chain reaction (PCR). At the time of tissue harvest, vessel walls were snap-frozen in liquid nitrogen and stored at −80°C. Later, the walls were resuspended and mechanically homogenized in TriPure Isolation Reagent (Roche). RNA was prepared using a Direct-zol RNA MiniPrep kit (Zymo Research) according to the instructions of the manufacturer. The RNA integrity number was >7 for all included samples. Complementary DNA was synthesized using Moloney murine leukemia virus reverse transcriptase (Invitrogen) and 200 ng of RNA, using a MyCycler thermocyler (Bio-Rad). Quantitative PCR was performed with SYBR Green PCR Master Mix (Qiagen) according to the instructions of the manufacturer and was carried out using an ABI PRISM 7900HT system (Applied Biosystems). Primers for mouse CXCL-1, CCL-2, interleukin-6, thrombomodulin, intercellular adhesion molecule 1, vascular cell adhesion molecule 1, E-selectin, and P-selectin were purchased from Qiagen (QuantiTect Primer Assays, which have proprietary primer sequences). The housekeeping gene was GAPDH, with primer sequences of 5′-ACCACAGTCCATGCCATCAC-3′ and 5′-TCCACCACCCTGTTGCTGTA-3′.

The threshold cycle (C_t) value was normalized to the C_t of GAPDH to obtain the ΔC_t. The $\Delta\Delta C_t$ values were then determined by comparing each ΔC_t to the average ΔC_t for the sham group treated with control IgG. Data were presented as the relative fold change, using the formula $2^{-\Delta\Delta C_t}$.

Flow cytometry and measurement of cell-free DNA. After lysing red blood cells (RBCs), total leukocytes were stained with anti–Ly-6G and anti-human IgG (BioLegend). Staining was performed for 30 minutes at 4°C. After washing, cells were fixed in 2% paraformaldehyde before analysis with a CyAn ADP Analyzer (Beckman Coulter). Further data analysis was performed using FlowJo.

Cell-free DNA was quantified in plasma using a Quant-iT PicoGreen dsDNA Assay Kit (Invitrogen) according to the instructions of the manufacturer.

Statistical analysis. GraphPad Prism software version 6 was used for data analysis. Normally distributed data were analyzed by unpaired *t*-test, and skewed data were assessed by Mann-Whitney test. The chi-square test was used to assess dichotomous variables (thrombosis frequency). *P* values less than 0.05 were considered significant.

Study approval. This study was reviewed and approved by the University of Michigan Institutional Review Board. Written informed consent was received from all participants prior to inclusion. The University of Michigan Institutional Animal Care and Use Committee approved all mouse protocols used in this study.

RESULTS

Development of larger thrombi following IVC stenosis in mice administered APS IgG. As detailed above, other investigators have shown that administration of APS IgG creates a prothrombotic milieu in mice. When

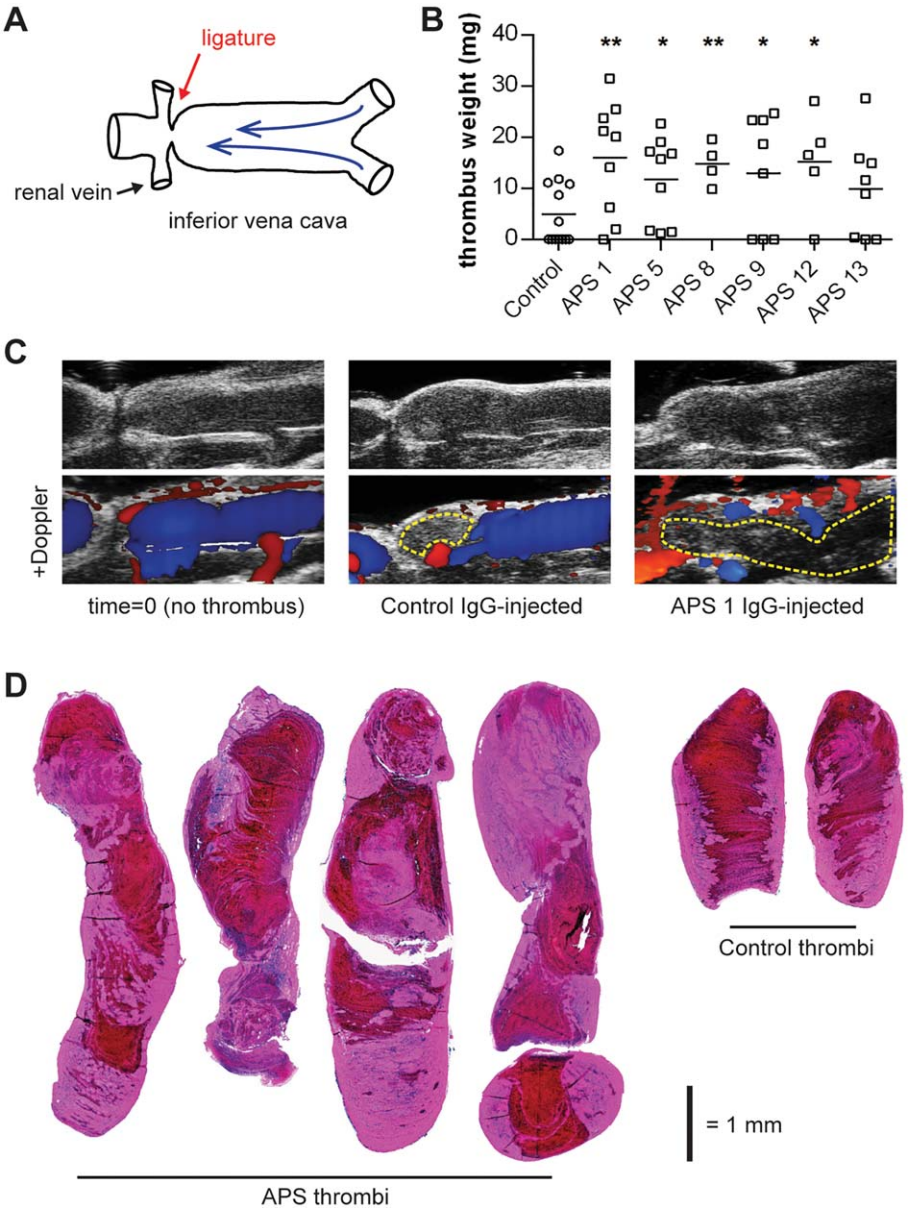

Figure 1. IgG from patients with antiphospholipid syndrome (APS IgG) promotes venous thrombosis in mice. **A,** Schematic drawing of the inferior vena cava (IVC) stenosis model, in which a ligature is fastened just distal to the renal veins to cause a consistent restriction in flow. **B,** Thrombus weight in control mice and mice administered APS IgG. IgG was purified from either APS patients 1, 5, 8, 9, 12, and 13 or healthy controls and administered to the mice (2 intraperitoneal injections, 48 hours apart). At the time of the second injection, the IVC was narrowed (stenosed), as described in **A**. Forty-eight hours later, the thrombus weight was measured. Each data point represents an individual mouse; horizontal lines show the mean. * = $P < 0.05$; ** = $P < 0.01$ versus control. **C,** Ultrasound images of the IVC at time 0 and 48 hours after injection of either control IgG or APS IgG. Red or blue indicates active flow. The dashed lines delineate areas in which flow is excluded due to thrombosis. Images are representative of those from 3 mice per group. **D,** Representative hematoxylin and eosin–stained thrombus sections from APS IgG–treated mice and control mice (images obtained with a 4× objective are stitched together). Among the APS thrombi, the 2 on the left are from the APS 1 group, and the 2 on the right are from the APS 5 group. Note the mix of red blood cell (RBC)–rich (red) and RBC-poor (pink) areas.

thrombosis is then triggered by a "second hit," APS mice develop thrombi more efficiently than controls. Here, we characterized 2 mouse models of venous thrombosis that have not been previously studied in the context of APS.

In the first model, the IVC is subjected to a reproducible, flow-restricting stenosis (Figure 1A), which leads to thrombosis in ~50% of control mice. This is referred to as a "flow restriction" or "stenosis" model (17,22,26). To

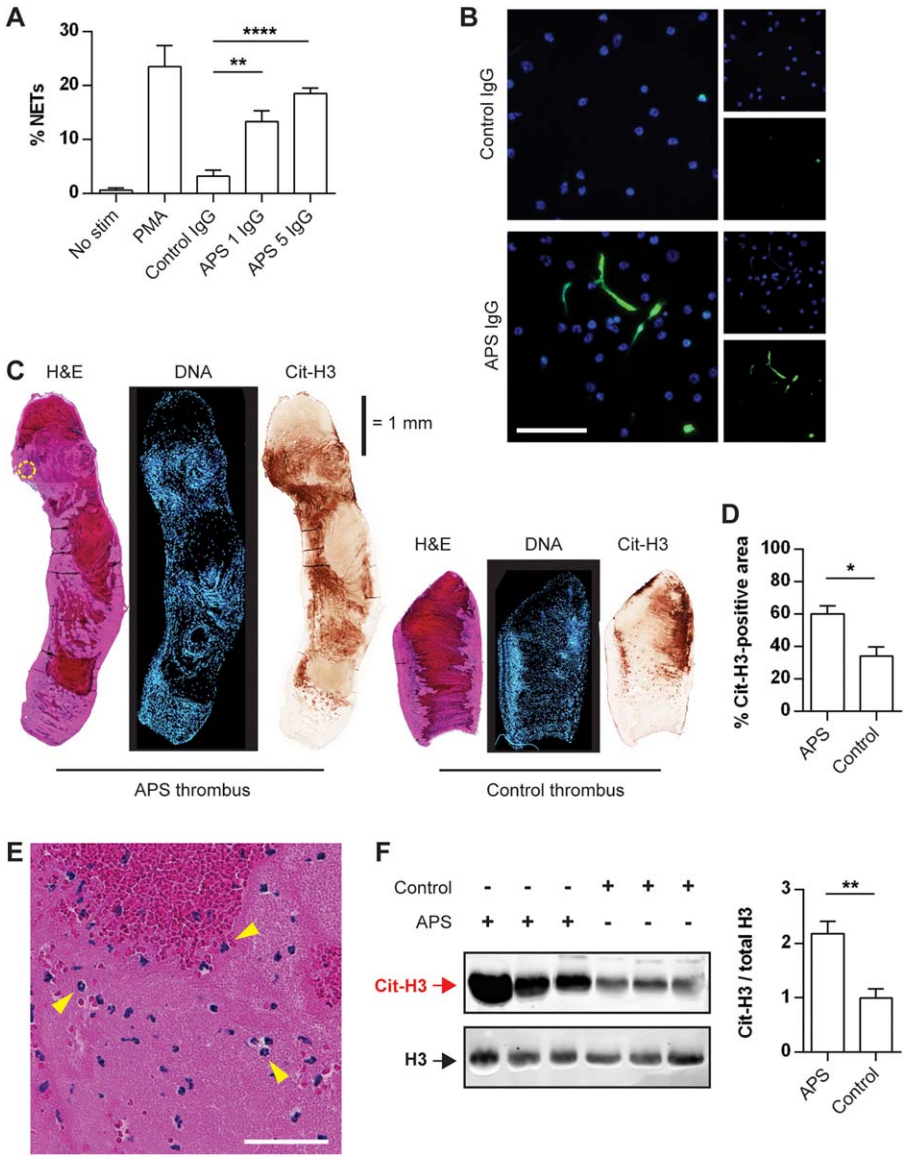

Figure 2. APS IgG promotes the release of neutrophil extracellular traps (NETs) in vitro and in vivo. **A,** Percentage of NETs in mouse neutrophils that were left unstimulated (no stim) or were stimulated with phorbol myristate acetate (PMA), control IgG, or APS IgG. Immunofluorescence microscopy was used to score NETosis. Values are the mean ± SEM (n = 4–6 per condition). **B,** Representative microscopic images from the immunofluorescence analysis described in **A**. Blue staining indicates DNA; green staining indicates citrullinated histone H3 (Cit-H3). NETs are shown as extracellular areas of blue and green overlap. Bar = 50μ. **C,** Staining of APS and control thrombus sections with hematoxylin and eosin (H&E), Hoechst 33342 (for DNA), and anti–Cit-H3 (for NETs) at the 48-hour time point. Staining is representative of that in 4 thrombus sections per group. **D,** Quantification of Cit-H3–positive surface area of the APS and control thrombus sections shown in **C**. Values are the mean ± SEM (n = 4 per group). **E,** Infiltration of neutrophils in regions prominently stained for Cit-H3. **Arrowheads** indicate 3 representative neutrophils (although essentially every cell in this field is a neutrophil). Bar = 50μ. **F,** Left, Western blots of total thrombus protein for Cit-H3 and total histone H3 (H3) in APS and control thrombi. Right, Quantification of Cit-H3/total H3 in APS and control thrombi. For APS thrombi, 3 were from the APS 1 group, and 3 were from the APS 5 group. Values are the mean ± SEM arbitrary units (n = 6 per group). * = $P < 0.05$; ** = $P < 0.01$; **** = $P < 0.0001$. See Figure 1 for other definitions.

test the role of APS IgG, we purified total IgG from 6 "triple-positive" patients with primary APS (positive for IgG anticardiolipin antibody, IgG anti-β_2GPI, and lupus anticoagulant), as well as total IgG from healthy volunteers. IgG from healthy volunteers was pooled to produce "control IgG," which was used as the control treatment for

all of the experiments. Wild-type C57BL/6 mice were then administered IgG by 2 intraperitoneal injections (500 μg each, 48 hours apart). At the time of the second IgG injection, stenosis was induced. Forty-eight hours later, thrombus weight was assessed (Figure 1B). As compared with control mice, APS IgG–treated mice formed significantly larger thrombi (Figures 1C and D). Hematoxylin and eosin (H&E) staining showed both RBC-rich and RBC-poor regions within thrombi, a feature that is typical of human deep vein thrombosis (DVT) (34), and which has been described by others in similar flow restriction models (17,22,26).

The second model differs from the stenosis model in that the IVC is fully ligated, along with ligation of all visible side and back branches. This is known as a "stasis" model (30). Resulting thrombi (the formation of which occurs >97% of the time in control mice) are significantly enriched in RBCs (30). It has also been reported that neutrophils and NETs play a relatively less important role in the stasis model as compared with 1) models utilizing flow restriction and 2) authentic human DVT (19,30). In contrast to the results of experiments with the stenosis model (Figure 1B), administration of APS IgG did not lead to significantly larger thrombi when mice were subjected to the stasis model (see Supplementary Figure 1, available on the *Arthritis & Rheumatology* web site at http://onlinelibrary.wiley.com/doi/10.1002/art.39938/abstract). These data demonstrate that treatment with APS IgG leads to larger thrombi in a model of venous flow restriction but not in a model of complete stasis. We therefore focused on the stenosis model for the following experiments.

Thrombi in mice administered APS IgG (APS thrombi) are enriched in NETs. Regarding the mechanism of APS IgG–accelerated thrombosis, we next sought to determine whether APS IgG could promote NETosis in vitro. We observed that, compared with control IgG, APS IgG stimulated mouse neutrophils to undergo NETosis (Figure 2A). As would be expected, these in vitro NETs had detectable DNA, Cit-H3, and myeloperoxidase (Figure 2B, and data not shown). Given that citrullinated histones are recognized as being the best biochemical marker of NETs, we extended our staining for Cit-H3 to thrombus sections. Although Cit-H3 was present in both APS and control thrombi, staining was especially widespread in APS thrombi (Figures 2C and D). When we analyzed corresponding H&E-stained sections, we observed that regions rich in Cit-H3 staining were infiltrated by neutrophils as the predominant nucleated cells (Figure 2E). Furthermore, quantification of Cit-H3 by Western blotting revealed significant enrichment of Cit-H3 in APS thrombi (Figure 2F). These data suggest that NETosis is exaggerated in the context of APS IgG treatment, both in vitro and in vivo.

Thrombosis in APS IgG–treated mice by 6 hours. In mice treated with APS IgG, thrombi developed by 6 hours. Because we were interested in whether NETs might play a role as initiators of thrombosis in APS, we turned our attention from the 48-hour time point (Figures 1 and 2) to the 6-hour time point. Furthermore, in these experiments, we added an additional control group (sham) in which a laparotomy was performed and the IVC was exposed, but without tying a stenosis-inducing ligature (see Supplementary Figure 2A, available on the *Arthritis & Rheumatology* web site at http://onlinelibrary.wiley.com/doi/10.1002/art.39938/abstract). As before, mice were treated with either control or APS IgG. No mouse in the sham group developed an IVC thrombus, even after administration of APS IgG. However, with stenosis, 50% of control IgG–treated mice and 100% of mice treated with APS IgG did develop thrombi at 6 hours (n = 10 per group (see Supplementary Figure 2B).

APS IgG binding of neutrophils in vivo. We first considered whether neutrophils might differ functionally between the 4 experimental conditions (control-sham, control-stenosis, APS-sham, APS-stenosis) (see Supplementary Figure 2A). We scored Ly-6G–positive neutrophils for surface binding of human IgG. Interestingly, we observed that mice in both the APS-sham and APS-stenosis groups were more likely to have human IgG bound to their neutrophils compared with controls (Figures 3A and B). As a surrogate for circulating NETs, we measured cell-free plasma DNA in the same mice. The only condition in which a statistically significant "spike" in cell-free DNA was observed was APS-stenosis (Figure 3C), albeit with notable variability between individual mice at the 6-hour time point. In summary, neutrophils from APS IgG–treated mice were more likely than controls to have human IgG on their surface. Furthermore, when these APS IgG–treated mice were subjected to IVC stenosis, they also demonstrated higher levels of cell-free DNA.

Similar numbers of total neutrophils in control IgG–treated mice and APS IgG–treated mice. At the 6-hour time point, we also quantified the numbers of neutrophils and platelets in the circulation (Figures 4A and B). While stenosis caused neutrophilia and thrombocytopenia as compared with the sham groups, control IgG–treated mice and APS IgG–treated mice did not differ in this regard. Furthermore, when we focused on the condition in which some mice formed thrombi and some did not (control-stenosis), the presence of a thrombus did not clearly predict either thrombocytopenia or neutrophilia (see Supplementary Figure 3, available on the

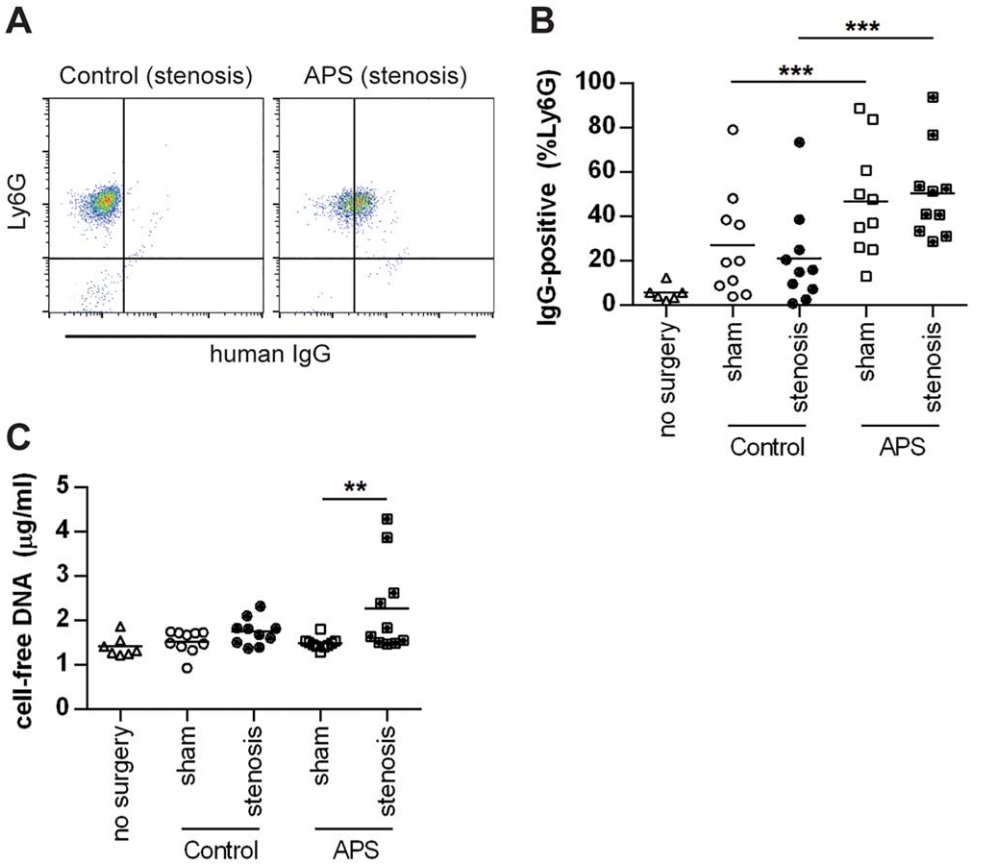

Figure 3. Mice treated with IgG from the APS 1 group have higher levels of neutrophil-bound IgG and cell-free DNA at 6 hours compared with mice treated with control IgG. Mice in both the sham groups and the stenosis groups underwent laparotomy, with exposure of the IVC; however, ligature was applied to the IVC only in mice in the stenosis groups. **A,** Representative histograms demonstrating staining for Ly-6G (a neutrophil marker) and human IgG, after gating for neutrophils by forward/side scatter. Ly-6G positivity was determined by flow cytometry in nucleated cells from peripheral blood. **B,** Percentage of Ly-6G–positive cells in the control-sham, control-stenosis, APS-sham, and APS-stenosis groups. **C,** Levels of cell-free DNA in the control-sham, control-stenosis, APS-sham, and APS-stenosis groups. In **B** and **C,** each data point represents an individual mouse; horizontal lines show the mean. ** = $P < 0.01$; *** = $P < 0.001$. See Figure 1 for definitions. Color figure can be viewed in the online issue, which is available at http://onlinelibrary.wiley.com/journal/doi/10.1002/art.39938/abstract.

Arthritis & Rheumatology web site at http://onlinelibrary.wiley.com/doi/10.1002/art.39938/abstract). In summary, although APS IgG–treated mice were at greater risk of thrombosis, this risk did not appear to be explained by the numbers of circulating neutrophils or platelets.

Vessel wall response to stenosis in control IgG–treated mice and APS IgG–treated mice. At the time when the mice were killed (6 hours after sham or stenosis procedure), we sampled a portion of the vessel wall just distal to the renal veins (in the region of the vessel where a thrombus formed in some mice). We then tested the expression of genes that may be indicative of vessel wall activation (Figures 4C and D, and Supplementary Figure 4, available on the *Arthritis & Rheumatology* web site at http://onlinelibrary.wiley.com/doi/10.1002/art.39938/abstract). Some genes, including intercellular adhesion molecule 1, vascular cell adhesion molecule 1, E-selectin, and P-selectin, were not regulated by any of the conditions (Supplementary Figure 4).

However, for other genes, including CXCL-1, CCL-2, interleukin-6, and thrombomodulin, 2 interesting trends were observed. First, when considering only the sham groups, there was up-regulation in APS IgG–treated mice compared with controls (Figures 4C and D and Supplementary Figure 4). Second, upon induction of stenosis, *both* APS IgG–treated mice and control mice demonstrated marked up-regulation compared with the sham groups, especially of CXCL-1 and CCL-2. Notably, APS IgG–treated mice and control mice did not differ in terms of the degree of this up-regulation (Figures 4C and D and Supplementary Figure 4). In parallel, we assessed whether the level of soluble P-selectin, which sometimes is used as a marker of endothelial activation, differed between the groups. When considering only the sham groups, P-selectin levels were higher in APS IgG–treated mice

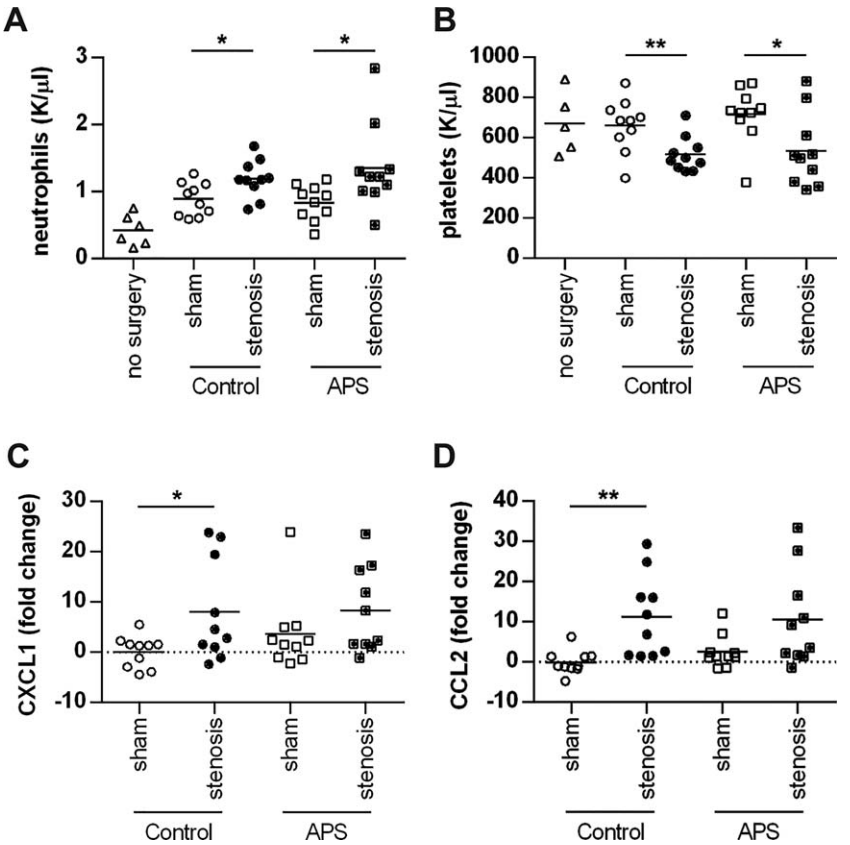

Figure 4. Mice treated with control IgG and those treated with IgG from the APS 1 group had similar numbers of circulating cells or markers of vessel wall activation at 6 hours. Mice in both the sham groups and the stenosis groups underwent laparotomy with exposure of the IVC; however, ligature was applied to the IVC only in mice in the stenosis groups. **A** and **B,** Neutrophil counts (**A**) and platelet counts (**B**) in peripheral blood from mice in the control-sham, control-stenosis, APS-sham, and APS-stenosis groups. **C** and **D,** Quantitative polymerase chain reaction analysis of genes that may indicate vessel wall activation. Portions of the vessel walls were obtained distal to the renal veins (in the region of the vessel where a thrombus formed in some mice). Mice in both the control-stenosis and APS-stenosis groups demonstrated up-regulation of CXCL-1 (**C**) and CCL-2 (**D**) compared with the sham groups. Each data point represents an individual mouse; horizontal lines show the mean. $* = P < 0.05$; $** = P < 0.01$. See Figure 1 for definitions.

compared with controls (Supplementary Figure 5, available on the *Arthritis & Rheumatology* eb site at http://onlinelibrary.wiley.com/doi/10.1002/art.39938/abstract). In contrast, upon stenosis, there was no difference between APS IgG–treated mice and control mice (Supplementary Figure 5).

In summary, we did observe subtle evidence of vessel wall activation upon administration of APS IgG compared with control IgG. However, this difference was overwhelmed by flow restriction (stenosis), which led to significant up-regulation of genes that track with vessel wall activation.

Presence of NETs in APS thrombi at 6 hours. At the 6-hour time point, we observed evidence of Cit-H3 staining of thrombi, which was focused at the periphery of the thrombus (where the thrombus was previously engaging the vessel wall) (Figures 5A and B and Supplementary Figure 6, available on the *Arthritis & Rheumatology* web site at http://onlinelibrary.wiley.com/doi/10.1002/art.39938/abstract). Furthermore, when assessed by Western blotting, Cit-H3 content was significantly increased in APS thrombi as compared with controls (Figure 5C). In summary, Cit-H3 content in APS thrombi was already exaggerated at 6 hours. Whether these NETs are released because of neutrophil contact with the vessel wall, or whether NETs may form elsewhere and then associate with the periphery of the thrombus, remains to be determined.

Abrogation of thrombosis in APS IgG–treated mice by both neutrophil depletion and DNase administration. Finally, we turned our attention to potential therapeutic approaches, testing them in control mice and APS IgG–treated mice at the 6-hour time point. Although there was a subtle trend toward efficacy, neither neutrophil depletion nor DNase treatment significantly reduced thrombosis in control mice (Figure 6A). In contrast, both treatments F6

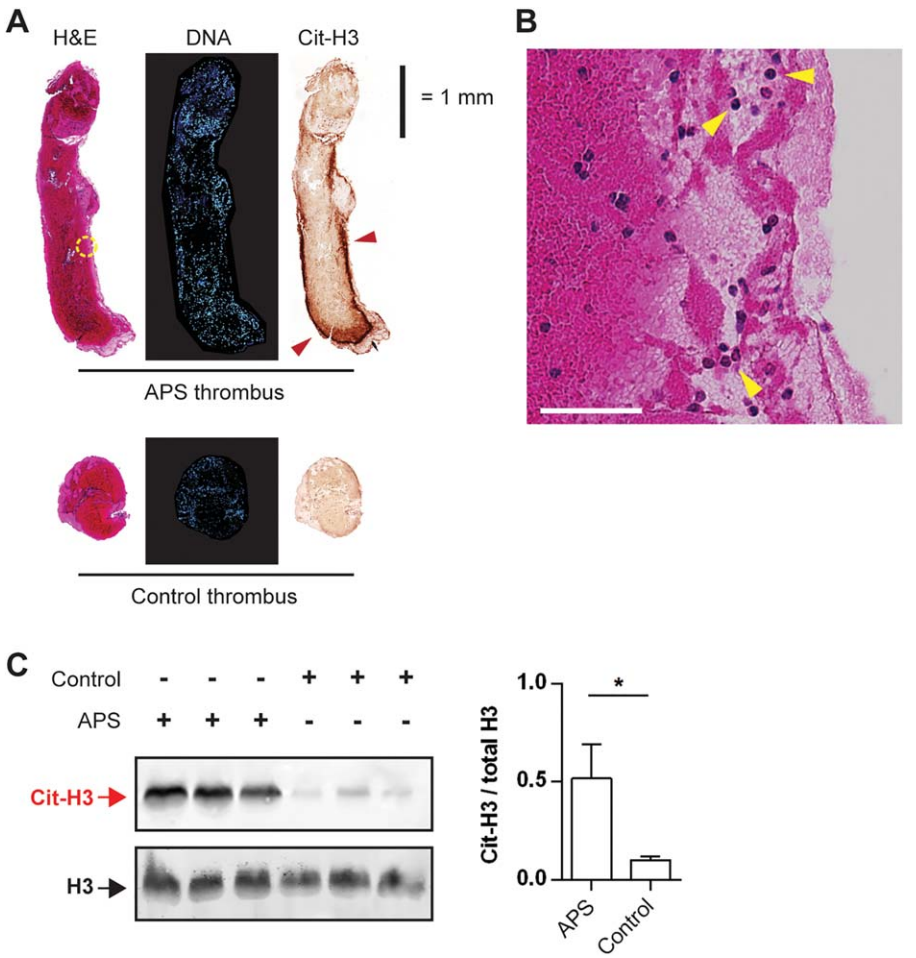

Figure 5. Thrombi from APS IgG–treated mice contain neutrophil extracellular traps (NETs) at 6 hours. All mice underwent the stenosis procedure. **A,** Thrombus sections were stained with hematoxylin and eosin (H&E), Hoechst 33342 (for DNA), and anti–citrullinated histone H3 (anti–Cit-H3). At 6 hours, the RBC-rich areas made up the majority of the thrombi, while the RBC-poor areas were largely confined to the periphery. **Arrowheads** indicate Cit-H3 staining, which was localized to the periphery (vessel wall interface) of the APS thrombus at the 6-hour time point. The dashed circle indicates an area that is shown at higher magnification in **B**. Staining is representative of 4 thrombi per group. **B,** Presence of NETs in an APS thrombus at 6 hours. **Arrowheads** indicate 3 representative neutrophils (although essentially every cell in this field is a neutrophil). Bar = 50 μ. **C,** Left, Western blots of total thrombus protein for citrullinated histone H3 (Cit-H3) and total histone H3 (H3). Right, Quantification of Cit-H3/total H3 in APS and control thrombi. For APS thrombi, 3 were from the APS 1 group, and 3 were from the APS 5 group. Values are the mean ± SEM arbitrary units (n = 6 per group). * = $P < 0.05$. See Figure 1 for other definitions.

resulted in a marked reduction of thrombosis in APS IgG–treated mice (Figures 6B and C). To examine the interconnectedness between neutrophil depletion and DNase treatment, we tested the thrombi of neutrophil-depleted mice for the presence of NETs. When APS thrombi form under baseline conditions, they are rich in both total histone H3 and Cit-H3 (Figure 5). Interestingly, we observed that both markers were essentially absent from the thrombi of neutrophil-depleted mice (Figure 6D). This supports the notion that neutrophils not only are the source of NETs but also are the primary nucleated cells infiltrating thrombi at the 6-hour time point. Importantly, the degree of neutrophil depletion did not differ between the groups (Figure 6E). In summary, it is noteworthy that APS IgG–treated mice that were treated with either DNase or neutrophil depletion became essentially indistinguishable from control mice (Figure 6F), emphasizing the importance of NETosis in the acceleration of thrombosis by APS IgG.

DISCUSSION

Recent studies by our group and others have suggested a role for NETosis in the thrombotic complications of APS (16–18,35,36). Exposure of neutrophils to antiphospholipid antibodies promotes NETosis (16), and when NETs form in patients with APS, they appear to be

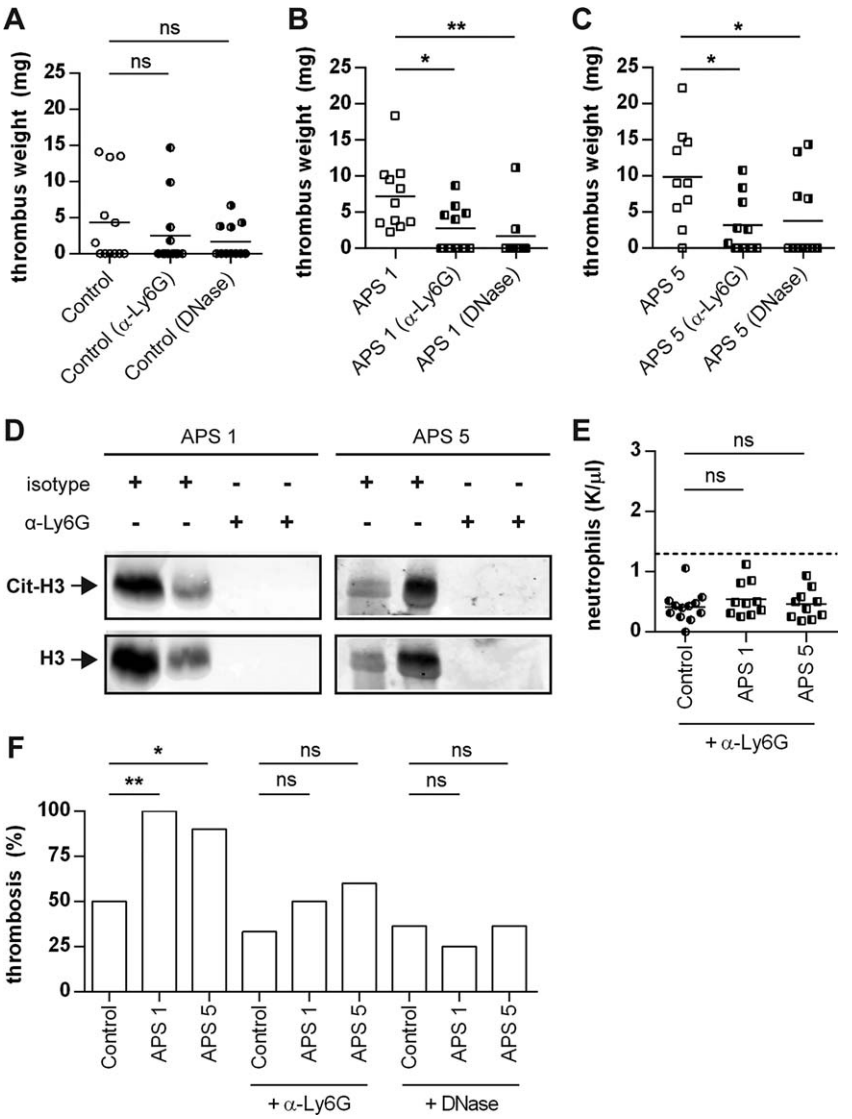

Figure 6. DNase administration and neutrophil depletion protect against APS IgG–accelerated thrombosis at 6 hours. Neutrophil depletion was performed with an anti–Ly-6G monoclonal antibody that was administered 24 hours before the first control or APS IgG injection. DNase was administered only once, immediately following the stenosis procedure. **A–C,** Thrombus weights in mice in each of the 9 treatment groups at 6 hours. Each data point represents an individual mouse; horizontal lines show the mean. **D,** Western blots of total thrombus protein for citrullinated histone H3 (Cit-H3) and total histone H3 (H3) in mice treated with isotype control and mice treated with anti–Ly-6G. The lanes were loaded with equal amounts of total protein. Neutrophil depletion reduced the neutrophil extracellular trap (NET) content of APS thrombi. Mice treated with control IgG had low NET content at baseline (see Figure 5C) and are not shown here. **E,** Level of neutrophil depletion in the control group, the APS 1 group, and the APS 5 group. The efficiency of neutrophil depletion did not differ between the groups. The dashed line represents the mean neutrophil count in mice in the control-stenosis group described in Figure 4A. **F**, Quantification of the data shown in A–C, presented as the thrombosis frequency and stratified by treatment group. $* = P < 0.05$; $** = P < 0.01$. NS = not significant (see Figure 1 for other definitions).

relatively resistant to degradation (17). APS NETs promote thrombin generation, an effect that can be blocked by treatment with DNase (16). It is also notable that low-density granulocytes, a subset of neutrophils that are prone to exaggerated NETosis, have recently been identified in patients with APS, especially in those with high titers of IgG anti-β_2GPI (18). Without a proven strategy for identifying low-density granulocytes in mice (and actually without proof that they exist at all in mice), low-density granulocytes were not considered as part of our studies. In the current study, we sought to develop an in vivo model that would allow us to assess the stimulation of

neutrophils by antiphospholipid antibodies in an environment that might recapitulate thrombus formation in humans.

Animal models have been an important tool in the APS field, in some instances leading to new considerations in patient care such as the use of hydroxychloroquine or complement inhibitors (7,37). In terms of assessing venous thrombosis, these models have typically relied on explicit vessel wall (and presumably endothelial) damage, which is not a usual part of human DVT (in which stagnant blood flow is a more important factor) (38). This study and the recent work of other investigators have suggested that the IVC stenosis model used in this study leads to a more subtle regulation of the vessel wall in response to disrupted flow (22).

We have shown for the first time that administration of IgG from patients with APS accelerates venous thrombosis in a flow restriction model, a phenotype that is associated with 1) human IgG binding to the neutrophil surface, 2) elevated levels of plasma cell–free DNA, and 3) increased infiltration of NETs into the thrombi themselves. These findings differ from those we observed in the "stasis" model of venous thrombosis, in which APS IgG demonstrated no clear phenotype with complete stasis. One might speculate that this relates to the relatively less important role of inflammatory cells (and perhaps especially neutrophils) under conditions of complete flow arrest (30). Indeed, other investigators have proposed that models that maintain flow are better mimickers of human DVT (19,22).

Heterotypic *inter*cellular interactions between primed neutrophils and activated platelets/endothelial cells have been recognized to facilitate NETosis in various systems (39–41). We speculate that antiphospholipid antibodies may prime neutrophils in vivo, but that a second signal (perhaps from the endothelium) is necessary for full activation to thromboinflammatory NETosis (Supplementary Figure 7, available on the *Arthritis & Rheumatology* web site at http://onlinelibrary.wiley.com/doi/10.1002/art.39938/abstract). This could be one reason for the sporadic nature of thrombi in patients with APS and might also explain our immunohistochemical data in which Cit-H3 staining localizes to the vessel wall interface of early thrombi. However, as pointed out above, we do not have real-time data to prove that these NETs were released at the vessel wall in situ. It is also possible that they formed elsewhere and then deposited along the activated endothelium. Further study with intravital microscopy is needed.

A recent study demonstrated that DNase may protect against venous thrombosis in control mice, utilizing a model of flow restriction that is similar to ours (26). This is in contrast to our data, in which we observed a statistically significant effect of DNase only in APS IgG–treated mice. Our experiments did differ from those in earlier studies in that we especially focused therapy on the early time point of 6 hours. It is possible that NETosis—perhaps triggered by the emerging thrombus itself—is a key regulator of thrombus propagation over time. Therefore, a therapeutic effect will be revealed only at later time points. In support of this hypothesis is our finding of very little Cit-H3 in control thrombi at 6 hours. This is in contrast to thrombi in APS IgG–treated mice, in which it was readily detectable at this early time point (Figure 5C). It should also be pointed out that the details of the model (including spacer size) were not identical between our study and the earlier work (26). It is certainly possible that the particulars of stenosis and flow have an impact on the degree of vessel wall activation and thrombus NET content.

There is a clear need in the APS field for precision treatments that address underlying pathophysiology. Presently, patients are treated with long-term anticoagulation, a therapy that carries inherent risk and is not uniformly effective (3). The possibility of DNase as a potential therapeutic agent in patients with SLE has long been considered (42–44); however, it is unclear whether sufficient and durable plasma levels can be achieved with currently available preparations. As mechanisms of NETosis become better understood, it may be possible to use agents such as peptidylarginine deiminase inhibitors or neutrophil elastase inhibitors to target the process of NETosis (45,46), or possibly anti-interferon drugs to target the downstream effects of NETs (47). In summary, we suggest that neutrophils should continue to be explored as therapeutic targets in APS. There is also a need to extend these studies to models beyond venous thrombosis, including arterial thrombosis and thrombosis in the microvasculature (10,15,48).

AUTHOR CONTRIBUTIONS

All authors were involved in drafting the article or revising it critically for important intellectual content, and all authors approved the final version to be published. Dr. Knight had full access to all of the data in the study and takes responsibility for the integrity of the data and the accuracy of the data analysis.

Study conception and design. Meng, Yalavarthi, Kanthi, Luke, Pinsky, Henke, Knight.

Acquisition of data. Meng, Yalavarthi, Kanthi, Mazza, Elfline.

Analysis and interpretation of data. Meng, Yalavarthi, Kanthi, Knight.

REFERENCES

1. Gomez-Puerta JA, Cervera R. Diagnosis and classification of the antiphospholipid syndrome. J Autoimmun 2014;48–49:20–5.
2. Bertolaccini ML, Amengual O, Andreoli L, Atsumi T, Chighizola CB, Forastiero R, et al. 14th International Congress on Antiphospholipid Antibodies Task Force: report on antiphospholipid syndrome laboratory diagnostics and trends [review]. Autoimmun Rev 2014;13:917–30.

3. Abreu MM, Danowski A, Wahl DG, Amigo MC, Tektonidou M, Pacheco MS, et al. The relevance of "non-criteria" clinical manifestations of antiphospholipid syndrome: 14th International Congress on Antiphospholipid Antibodies Technical Task Force report on antiphospholipid syndrome clinical features [review]. Autoimmun Rev 2015;14:401–14.
4. Willis R, Harris EN, Pierangeli SS. Pathogenesis of the antiphospholipid syndrome. Semin Thromb Hemost 2012;38:305–21.
5. Pericleous C, Ruiz-Limon P, Romay-Penabad Z, Marin AC, Garza-Garcia A, Murfitt L, et al. Proof-of-concept study demonstrating the pathogenicity of affinity-purified IgG antibodies directed to domain I of β2-glycoprotein I in a mouse model of anti-phospholipid antibody-induced thrombosis. Rheumatology (Oxford) 2015;54:722–7.
6. Pierangeli SS, Vega-Ostertag ME, Raschi E, Liu X, Romay-Penabad Z, de Micheli V, et al. Toll-like receptor and antiphospholipid mediated thrombosis: in vivo studies. Ann Rheum Dis 2007;66:1327–33.
7. Pierangeli SS, Girardi G, Vega-Ostertag M, Liu X, Espinola RG, Salmon J. Requirement of activation of complement C3 and C5 for antiphospholipid antibody–mediated thrombophilia. Arthritis Rheum 2005;52:2120–4.
8. Arad A, Proulle V, Furie RA, Furie BC, Furie B. β_2-glycoprotein-1 autoantibodies from patients with antiphospholipid syndrome are sufficient to potentiate arterial thrombus formation in a mouse model. Blood 2011;117:3453–9.
9. Proulle V, Furie RA, Merrill-Skoloff G, Furie BC, Furie B. Platelets are required for enhanced activation of the endothelium and fibrinogen in a mouse thrombosis model of APS. Blood 2014;124:611–22.
10. Laplante P, Fuentes R, Salem D, Subang R, Gillis MA, Hachem A, et al. Antiphospholipid antibody-mediated effects in an arterial model of thrombosis are dependent on Toll-like receptor 4. Lupus 2016;25:162–76.
11. Cervera R, Piette JC, Font J, Khamashta MA, Shoenfeld Y, Camps MT, et al. Antiphospholipid syndrome: clinical and immunologic manifestations and patterns of disease expression in a cohort of 1,000 patients. Arthritis Rheum 2002;46:1019–27.
12. Ruiz-Irastorza G, Crowther M, Branch W, Khamashta MA. Antiphospholipid syndrome. Lancet 2010;376:1498–509.
13. Giannakopoulos B, Krilis SA. The pathogenesis of the antiphospholipid syndrome. N Engl J Med 2013;368:1033–44.
14. Meroni PL, Borghi MO, Raschi E, Tedesco F. Pathogenesis of antiphospholipid syndrome: understanding the antibodies. Nat Rev Rheumatol 2011;7:330–9.
15. Fischetti F, Durigutto P, Pellis V, Debeus A, Macor P, Bulla R, et al. Thrombus formation induced by antibodies to β2-glycoprotein I is complement dependent and requires a priming factor. Blood 2005; 106:2340–6.
16. Yalavarthi S, Gould TJ, Rao AN, Mazza LF, Morris AE, Nunez-Alvarez C, et al. Release of neutrophil extracellular traps by neutrophils stimulated with antiphospholipid antibodies: a newly identified mechanism of thrombosis in the antiphospholipid syndrome. Arthritis Rheumatol 2015;67:2990–3003.
17. Leffler J, Stojanovich L, Shoenfeld Y, Bogdanovic G, Hesselstrand R, Blom AM. Degradation of neutrophil extracellular traps is decreased in patients with antiphospholipid syndrome. Clin Exp Rheumatol 2014;32: 66–70.
18. Van den Hoogen LL, Fritsch-Stork RD, van Roon JA, Radstake TR. Low-density granulocytes are increased in antiphospholipid syndrome and are associated with anti–β_2-glycoprotein I antibodies: comment on the article by Yalavarthi et al [letter]. Arthritis Rheumatol 2016;68:1320–1.
19. Martinod K, Wagner DD. Thrombosis: tangled up in NETs. Blood 2014;123:2768–76.
20. Brinkmann V, Reichard U, Goosmann C, Fauler B, Uhlemann Y, Weiss DS, et al. Neutrophil extracellular traps kill bacteria. Science 2004;303:1532–5.
21. Brinkmann V, Zychlinsky A. Neutrophil extracellular traps: is immunity the second function of chromatin? J Cell Biol 2012;198:773–83.
22. Von Bruhl ML, Stark K, Steinhart A, Chandraratne S, Konrad I, Lorenz M, et al. Monocytes, neutrophils, and platelets cooperate to initiate and propagate venous thrombosis in mice in vivo. J Exp Med 2012;209:819–35.
23. Gould TJ, Vu TT, Swystun LL, Dwivedi DJ, Mai SH, Weitz JI, et al. Neutrophil extracellular traps promote thrombin generation through platelet-dependent and platelet-independent mechanisms. Arterioscler Thromb Vasc Biol 2014;34:1977–84.
24. Fuchs TA, Brill A, Duerschmied D, Schatzberg D, Monestier M, Myers DD Jr, et al. Extracellular DNA traps promote thrombosis. Proc Natl Acad Sci U S A 2010;107:15880–5.
25. Kambas K, Mitroulis I, Apostolidou E, Girod A, Chrysanthopoulou A, Pneumatikos I, et al. Autophagy mediates the delivery of thrombogenic tissue factor to neutrophil extracellular traps in human sepsis. PLoS One 2012;7:e45427.
26. Brill A, Fuchs TA, Savchenko AS, Thomas GM, Martinod K, de Meyer SF, et al. Neutrophil extracellular traps promote deep vein thrombosis in mice. J Thromb Haemost 2012;10:136–44.
27. Miyakis S, Lockshin MD, Atsumi T, Branch DW, Brey RL, Cervera R, et al. International consensus statement on an update of the classification criteria for definite antiphospholipid syndrome (APS). J Thromb Haemost 2006;4:295–306.
28. Hochberg MC. Updating the American College of Rheumatology revised criteria for the classification of systemic lupus erythematosus [letter]. Arthritis Rheum 1997;40:1725.
29. Pengo V, Tripodi A, Reber G, Rand JH, Ortel TL, Galli M, et al. Update of the guidelines for lupus anticoagulant detection. J Thromb Haemost 2009;7:1737–40.
30. El-Sayed OM, Dewyer NA, Luke CE, Elfline M, Laser A, Hogaboam C, et al. Intact Toll-like receptor 9 signaling in neutrophils modulates normal thrombogenesis in mice. J Vasc Surg 2016;64:1450–8.
31. Kanthi Y, Hyman MC, Liao H, Baek AE, Visovatti SH, Sutton NR, et al. Flow-dependent expression of ectonucleotide tri(di)-phosphohydrolase-1 and suppression of atherosclerosis. J Clin Invest 2016;64:1450–8.
32. Knight JS, Zhao W, Luo W, Subramanian V, O'Dell AA, Yalavarthi S, et al. Peptidylarginine deiminase inhibition is immunomodulatory and vasculoprotective in murine lupus. J Clin Invest 2013;123:2981–93.
33. Knight JS, Subramanian V, O'Dell AA, Yalavarthi S, Zhao W, Smith CK, et al. Peptidylarginine deiminase inhibition disrupts NET formation and protects against kidney, skin and vascular disease in lupus-prone MRL/lpr mice. Ann Rheum Dis 2015;74: 2199–206.
34. Sevitt S. The structure and growth of valve-pocket thrombi in femoral veins. J Clin Pathol 1974;27:517–28.
35. Duarte JH. Connective tissue diseases: neutrophil extracellular traps: a mechanism of thrombosis in patients with antiphospholipid syndrome? Nat Rev Rheum 2015;11:444.
36. Rao AN, Kazzaz NM, Knight JS. Do neutrophil extracellular traps contribute to the heightened risk of thrombosis in inflammatory diseases? World J Cardiol 2015;7:829–42.
37. Edwards MH, Pierangeli S, Liu X, Barker JH, Anderson G, Harris EN. Hydroxychloroquine reverses thrombogenic properties of antiphospholipid antibodies in mice. Circulation 1997;96:4380–4.
38. Esmon CT. Basic mechanisms and pathogenesis of venous thrombosis. Blood Rev 2009;23:225–9.
39. Clark SR, Ma AC, Tavener SA, McDonald B, Goodarzi Z, Kelly MM, et al. Platelet TLR4 activates neutrophil extracellular traps to ensnare bacteria in septic blood. Nat Med 2007;13:463–9.
40. Caudrillier A, Kessenbrock K, Gilliss BM, Nguyen JX, Marques MB, Monestier M, et al. Platelets induce neutrophil extracellular traps in transfusion-related acute lung injury. J Clin Invest 2012; 122:2661–71.
41. Gupta AK, Joshi MB, Philippova M, Erne P, Hasler P, Hahn S, et al. Activated endothelial cells induce neutrophil extracellular

traps and are susceptible to NETosis-mediated cell death. FEBS Lett 2010;584:3193–7.
42. Verthelyi D, Dybdal N, Elias KA, Klinman DM. DNAse treatment does not improve the survival of lupus prone (NZB × NZW)F1 mice. Lupus 1998;7:223–30.
43. Macanovic M, Sinicropi D, Shak S, Baughman S, Thiru S, Lachmann PJ. The treatment of systemic lupus erythematosus (SLE) in NZB/W F1 hybrid mice: studies with recombinant murine DNase and with dexamethasone. Clin Exp Immunol 1996; 106:243–52.
44. Davis JC Jr, Manzi S, Yarboro C, Rairie J, McInnes I, Averthelyi D, et al. Recombinant human DNase I (rhDNase) in patients with lupus nephritis. Lupus 1999;8:68–76.
45. Martinod K, Demers M, Fuchs TA, Wong SL, Brill A, Gallant M, et al. Neutrophil histone modification by peptidylarginine deiminase 4 is critical for deep vein thrombosis in mice. Proc Natl Acad Sci U S A 2013;110:8674–9.
46. Cools-Lartigue J, Spicer J, McDonald B, Gowing S, Chow S, Giannias B, et al. Neutrophil extracellular traps sequester circulating tumor cells and promote metastasis. J Clin Invest 2013. E-pub ahead of print.
47. Grenn RC, Yalavarthi S, Gandhi AA, Kazzaz NM, Nunez-Alvarez C, Hernandez-Ramirez D, et al. Endothelial progenitor dysfunction associates with a type I interferon signature in primary antiphospholipid syndrome. Ann Rheum Dis 2016. E-pub ahead of print.
48. Thalin C, Demers M, Blomgren B, Wong SL, von Arbin M, von Heijne A, et al. NETosis promotes cancer-associated arterial microthrombosis presenting as ischemic stroke with troponin elevation. Thromb Res 2016;139:56–64.